AIP | Review of Scientific Instruments

Note: A monoenergetic proton backlighter for the National Ignition Facility

J. R. Rygg, A. B. Zylstra, F. H. Séguin, S. LePape, B. Bachmann, R. S. Craxton, E. M. Garcia, Y. Z. Kong, M. Gatu-Johnson, S. F. Khan, B. J. Lahmann, P. W. McKenty, R. D. Petrasso, H. G. Rinderknecht, M. J. Rosenberg, D. B. Sayre, and H. W. Sio

Citation: Review of Scientific Instruments **86**, 116104 (2015); doi: 10.1063/1.4935581
View online: http://dx.doi.org/10.1063/1.4935581
View Table of Contents: http://scitation.aip.org/content/aip/journal/rsi/86/11?ver=pdfcov
Published by the AIP Publishing

Note: A monoenergetic proton backlighter for the National Ignition Facility

J. R. Rygg,[1] A. B. Zylstra,[2,a)] F. H. Séguin,[2] S. LePape,[1] B. Bachmann,[1] R. S. Craxton,[3] E. M. Garcia,[3] Y. Z. Kong,[3] M. Gatu-Johnson,[2] S. F. Khan,[1] B. J. Lahmann,[2] P. W. McKenty,[3] R. D. Petrasso,[2] H. G. Rinderknecht,[1,2] M. J. Rosenberg,[2,3] D. B. Sayre,[1] and H. W. Sio[2]
[1]*Lawrence Livermore National Laboratory, Livermore, California 94551, USA*
[2]*Plasma Science and Fusion Center, Massachusetts Institute of Technology, Cambridge, Massachusetts 02139, USA*
[3]*Laboratory for Laser Energetics, University of Rochester, Rochester, New York 14623, USA*

(Received 4 September 2015; accepted 26 October 2015; published online 12 November 2015)

A monoenergetic, isotropic proton source suitable for proton radiography applications has been demonstrated at the National Ignition Facility (NIF). A deuterium and helium-3 gas-filled glass capsule was imploded with 39 kJ of laser energy from 24 of NIF's 192 beams. Spectral, spatial, and temporal measurements of the 15-MeV proton product of the ^{3}He(d, p)^{4}He nuclear reaction reveal a bright (10^{10} protons/sphere), monoenergetic ($\Delta E/E = 4\%$) spectrum with a compact size (80 μm) and isotropic emission (~13% proton fluence variation and <0.4% mean energy variation). Simultaneous measurements of products produced by the D(d,p)T and D(d,n)^{3}He reactions also show 2×10^{10} isotropically distributed 3-MeV protons. [http://dx.doi.org/10.1063/1.4935581]

Since the pioneering work near the turn of the century,[1–4] proton radiography has been used to diagnose mass and electromagnetic field distributions in a variety of laser-generated plasma configurations. Mono-energetic proton radiography[5,6] in particular has been used extensively to provide quantitative information on diverse phenomena including laser-foil interactions,[7,8] magnetic reconnection,[9,10] magnetic flux compression,[11] the Rayleigh-Taylor instability,[12] the Weibel instability,[13] inertial confinement fusion (ICF) implosions,[14–16] indirect-drive ICF hohlraums,[17,18] and charged-particle stopping-power in warm dense matter.[19]

Commissioning a mono-energetic proton radiography platform at the National Ignition Facility (NIF)[20] would enable leveraging these diagnostic techniques on the larger and more extreme plasmas that can be generated by the NIF's 1.8 MJ laser energy. The precision of this platform depends on generating and characterizing a proton source of suitable properties. Mono-energetic proton sources have been well-characterized at the OMEGA laser facility,[21] and generation of protons at the NIF has been demonstrated using all 192 NIF beams.[22] This note reports the spectral, spatial, and temporal measurements of 15 MeV proton emission from a capsule implosion using only 24 beams at the NIF, which leaves 168 beams in reserve to drive a subject target.

The capsule consists of a 3 μm thick, 866 μm diameter SiO_2 spherical shell filled with a 1.74 mg/cm^3 gas mixture of deuterium (D_2) and helium-3 (40 at. % ^{3}He). The capsule was directly driven with 24 beams from 6 of NIF's 48 laser quads, with three quads from each hemisphere.[23,24] The primary laser pulse (Fig. 1) consisted of a 39.1 kJ, 52.8 TW peak, approximately 1 ns in duration.[25]

Explosion of the glass shell in response to the incident laser energy launches a shock inwards, heating the D^{3}He gas to multi-keV temperatures (1 keV = 1.16×10^7 K), and inducing nuclear production. In particular, the ^{3}He(d, p)^{4}He and D(d,p)T nuclear reactions,

$$D + {}^3He \rightarrow {}^4He + p + 18.35\ MeV, \quad (1)$$

$$D + D \rightarrow T + p + 4.03\ MeV, \quad (2)$$

produce protons with nominal birth energies of 14.63 MeV and 3.02 MeV, respectively.

The D^{3}He-proton spectrum emitted from the capsule was measured simultaneously along several directions with multiple wedge-range-filter (WRF) proton spectrometers[26–28] as well as by the magnetic recoil spectrometer (MRS).[29] The spectra (example in Fig. 2) are all well fit by Gaussian distributions. The average fit parameters give an integrated yield of $9.2 \pm 0.5 \times 10^9$ protons (inferred over 4π steradians), a mean energy of 14.981 ± 0.036 MeV, and a sigma of 0.283 ± 0.003 MeV (after subtracting the instrumental broadening of 0.180 MeV). The spectral width is thus very narrow, with full-width at half maximum over mean energy $\Delta E/E = 4.4\% \pm 0.1\%$. The mean energy is upshifted from the nominal value due to a thermal contribution (~60 keV) and due to charging of the capsule while the laser is on[30] (net 290 keV after any downshift while exiting the capsule).

The standard deviation in the D^{3}He proton yield along the different lines of sight was 13% (Fig. 3); such yield variations are typical when protons are emitted while the laser is on due to electromagnetic fields in the surrounding plasma.[14,16] The standard deviation of the mean energy along the different lines of sight is 55 keV, which, within the uncertainty, is consistent with isotropic mean proton energy.

Protons produced by the D(d,p)T reaction (DD-p) were measured along three directions with step-range filter

[a)]Present address: Los Alamos National Laboratory, Los Alamos, New Mexico 87545, USA.

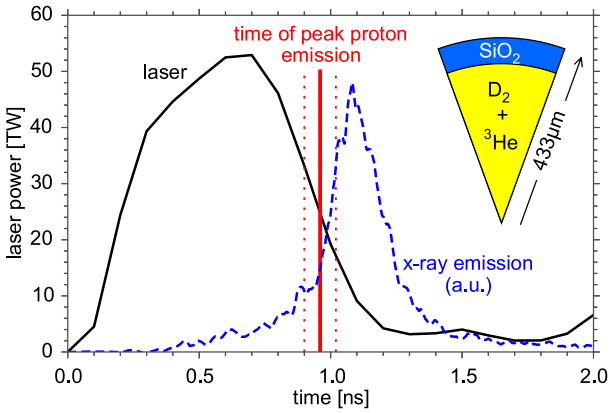

FIG. 1. A SiO_2 spherical shell filled with D_2 and ^3He gas [inset] was driven with a ~1 ns, 39 kJ laser pulse (NIF shot N150326). Peak 15 MeV proton emission is measured to occur at 0.96 ± 0.06 ns. A sharp peak (0.18 ns full width at half maximum (FWHM)) in x-ray emission from the imploded capsule comes in somewhat later at 1.10 ns, on top of a broader emission pedestal (0.75 ns FWHM).

detectors.[31] The weighted average DD-p yield was $2.27 \pm 0.06 \times 10^{10}$, with a 4% standard deviation between views. Neutrons produced by the D(d,n)^{3}He reaction (DD-n) were measured by several nTOF diagnostics.[32] The observed $2.5 \pm 0.25 \times 10^{10}$ neutron yield is consistent with the proton measurements and the 5% higher probability of the neutron branch of the DD reaction at a temperature of 11 keV.

The nTOF diagnostics also infer the DD-n burn-averaged ion temperature from the time-broadening of neutron arrival at the detector, giving 10.8 ± 0.8 keV. The D^{3}He burn-averaged ion temperature can likewise be estimated from the width of the proton spectrum,[33] giving 13.7 ± 0.3 keV (neglecting other broadening mechanisms). An alternative method of determining ion temperature is the yield ratio method.[33] Using the known 40 at. % ^{3}He composition gives 12.5 ± 0.5 keV for the D^{3}He vs DD-n yield, and 12.7 ± 0.3 keV for the D^{3}He vs DD-p yield. The systematic difference between these ion temperatures has been discussed previously[33] and is due in part to the different weighting of the temperature profile by the DD and D^{3}He nuclear production.

The time of D^{3}He proton emission was measured with the mag-pTOF diagnostic,[34,35] which observed a proton bangtime

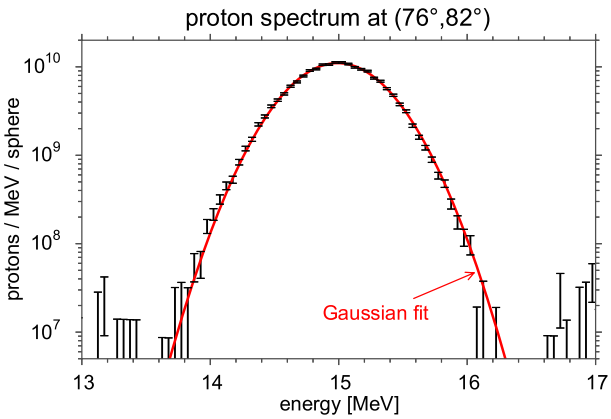

FIG. 2. The measured proton spectrum is well fit by a Gaussian distribution. Fit parameters for different lines of sight are shown in Fig. 3.

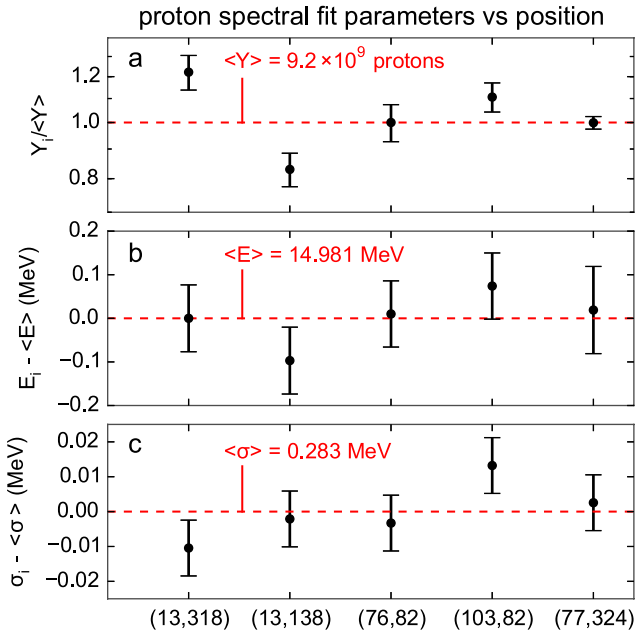

FIG. 3. Gaussian fit parameters of 15 MeV proton spectra vs detector position (listed as polar-azimuthal angles in target chamber) compared to the weighted mean of all detector results (horizontal dashed line). The measurement at (77,324) used the magnet-based MRS detector, all other measurements used WRF spectrometers. The reported linewidth sigmas have been corrected for instrumental broadening.

of 0.96 ± 0.06 ns (Fig. 1). This value includes consideration of the proton time-of-flight from the source to the detector using the proton spectrum measured on a nearby spectrometer. The temporal emission history of x-rays ($h\nu > 8$ keV) was measured with a streaked x-ray diagnostic.[36] The x-ray emission history has a sharp peak at 1.10 ± 0.03 ns on top of a broader pedestal. The sharp peak has a FWHM of 0.18 ± 0.05 ns, and the broader pedestal has a FWHM of about 0.75 ns. Protons are emitted primarily near the time of peak gas temperature, whereas the x-ray emission peaks ~140 ps later as some of the glass shell enters and cools the hot spot. This relative timing is consistent with earlier observations.[22]

The spatial profile of D^{3}He proton emission was measured with a variant of the proton penumbral imaging setup fielded previously at the OMEGA laser.[37–39] In this case, two orthogonal images were obtained simultaneously: one along the polar axis ($\theta = 0°$), and one along an equatorial axis ($\theta = 90°$, $\varphi = 78.75°$). A 2.8 (2.0) mm diameter circular aperture was located 100 (80) mm from the target along the polar (equatorial) axis, giving a geometric magnification of 11× (14×) when imaged onto the 100 × 100 mm square CR-39[26] detectors.

The setup was further modified from the previous implementation by the insertion of a 100 ×100 mm square of Fuji™ BAS-MS image plate[40] just behind the CR-39. This enables simultaneous measurement of the x-ray emission profile through the same apertures used for proton imaging. Filtration of the x-rays by 0.025 mm of Zr, 3.0 mm of CR-39, and 0.2 mm of Al passes an x-ray spectral band of 13-17 keV onto the image plates.

Surface brightness reconstructions[37,41] of the proton and x-ray penumbral images along the polar and equatorial views

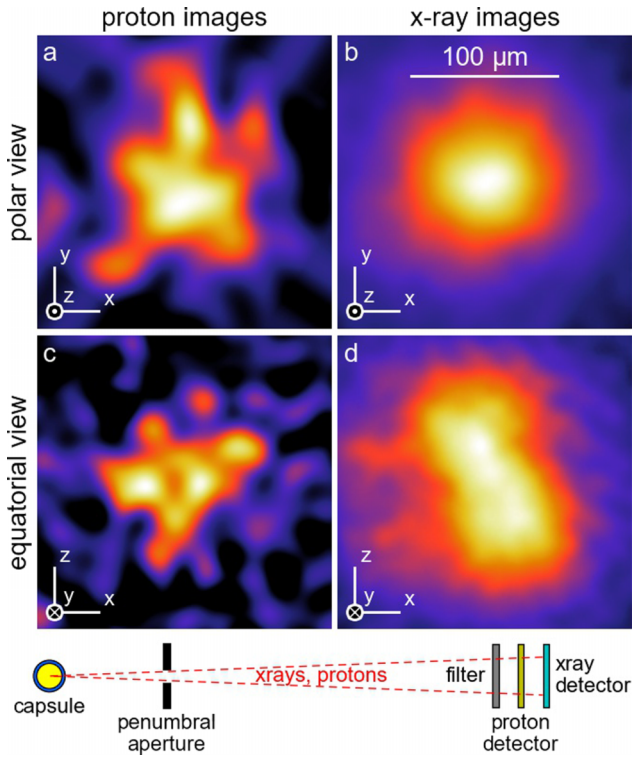

FIG. 4. Proton (15 MeV) and x-ray (13-17 keV) emission images as processed from two penumbral imaging systems along the polar and equatorial directions. Coordinates for each view are indicated in the lower left, where the (polar, azimuthal) angles of unit vectors are x = (90,169), y = (90,259), z = (0,0). Image sizes are all 200 μm square. The dominant noise spatial frequency of ~25 μm in the proton images is a byproduct of smoothing needed to overcome the relatively lower proton statistics.[37]

are shown in Fig. 4. Proton and x-ray emissions along the polar axis are close to round, with an azimuthally averaged FWHM diameter of 86 ± 22 μm and 79 ± 5 μm, respectively. The relatively lower proton statistics makes the proton emission size more uncertain. Proton and x-ray emissions along the equator are not as round, with the x-ray shape having +18 μm amplitude of Legendre mode P_2 (prolate), and the proton shape showing −20 μm P_2 amplitude (oblate). The spherically averaged sizes in the equatorial direction are 72 ± 16 μm and 90 ± 6 μm for the proton and x-ray emission, respectively. Pinhole images surrounding the main penumbral image confirm the size and shape of the x-ray emitting region.

Two-dimensional hydrodynamic simulations indicate that the implosion topology consists of a hot proton-emitting toroidal gas centered by a dense x-ray emitting core, qualitatively consistent with the images seen in Fig. 4. However, more detailed comparisons require 3-D simulations due to the azimuthal asymmetry of the irradiation pattern.

Upcoming NIF experiments will assess the dependence of performance characteristics such as proton yield and emission source size on various targets and laser parameters such as capsule diameter, drive energy, and drive symmetry.

In summary, an isotropic source of mono-energetic 15 MeV and 3 MeV protons has been extensively characterized with spectral, spatial, and temporal diagnostics at the National Ignition Facility. Only a fraction of NIF's 192 beams is needed to generate this proton source; the remainder is available to drive various subject plasmas for interrogation with the proton radiography technique.

The authors thank the NIF scientific, engineering, and operational staff for critical assistance in fielding this experiment and for these first steps in commissioning a proton radiography platform for the NIF. This work was performed under the auspices of the U.S. Department of Energy by Lawrence Livermore National Laboratory under Contract No. DE-AC52-07NA27344.

[1]N. S. P. King *et al.*, Nucl. Instrum. Methods Phys. **414**, 84 (1999).
[2]M. Borghesi *et al.*, Phys. Plasmas **9**, 2214 (2002).
[3]J. A. Cobble *et al.*, J. Appl. Phys. **92**, 1775 (2002).
[4]A. J. Mackinnon *et al.*, Rev. Sci. Instrum. **75**, 3531 (2004).
[5]C. K. Li *et al.*, Rev. Sci. Instrum. **77**, 10E725 (2006).
[6]N. L. Kugland *et al.*, Rev. Sci. Instrum. **83**, 101301 (2012).
[7]C. K. Li *et al.*, Phys. Rev. Lett. **97**, 135003 (2006).
[8]R. D. Petrasso *et al.*, Phys. Rev. Lett. **103**, 085001 (2009).
[9]C. K. Li *et al.*, Phys. Rev. Lett. **99**, 055001 (2007).
[10]M. Rosenberg *et al.*, Nat. Commun. **6**, 6190 (2015).
[11]O. V. Gotchev *et al.*, Phys. Rev. Lett. **103**, 215004 (2009).
[12]M. J.-E. Manuel *et al.*, Phys. Rev. Lett. **108**, 255006 (2012).
[13]C. M. Huntington *et al.*, Nat. Phys. **11**, 173 (2015).
[14]J. R. Rygg *et al.*, Science **319**, 1223 (2008).
[15]C. K. Li *et al.*, Phys. Rev. Lett. **100**, 225001 (2008).
[16]F. H. Séguin *et al.*, Phys. Plasmas **19**, 012701 (2012).
[17]C. K. Li *et al.*, Phys. Rev. Lett. **102**, 205001 (2009).
[18]C. K. Li *et al.*, Phys. Rev. Lett. **108**, 025001 (2012).
[19]A. B. Zylstra *et al.*, Phys. Rev. Lett. **114**, 215002 (2015).
[20]G. H. Miller, E. I. Moses, and C. R. Wuest, Opt. Eng. **43**, 2841 (2004).
[21]M. J.-E. Manuel *et al.*, Rev. Sci. Instrum. **83**, 063506 (2012).
[22]M. J. Rosenberg *et al.*, Phys. Plasmas **21**, 122712 (2014).
[23]The specific drive quads were Q12T, Q25T, Q35T, Q22B, Q35B, and Q46B. All beams used ~1mm NIF indirect-drive phase plates and were operated at best focus. The pointing strategy followed that described in Ref. 24, wherein one beam from each quad was pointed to the nearest pole and the other three were pointed in the vicinity of the equator.
[24]Y. Kong, Laboratory for Laser Energetics Document No. DOE/NA/1944-1159, 2014.
[25]The main pulse was followed 2 ns later by a 34 kJ, 20 TW "post-pulse" to deplete the NIF laser amplifiers. A new amplifier configuration has since been commissioned such that this post pulse is no longer required.
[26]F. H. Séguin *et al.*, Rev. Sci. Instrum. **74**, 975 (2003).
[27]F. H. Séguin *et al.*, Rev. Sci. Instrum. **83**, 10D908 (2012).
[28]A. B. Zylstra *et al.*, Rev. Sci. Instrum. **83**, 10D901 (2012).
[29]J. A. Frenje *et al.*, Rev. Sci. Instrum. **79**, 10E502 (2008).
[30]D. G. Hicks *et al.*, Phys. Plasmas **7**, 5106 (2000).
[31]M. J. Rosenberg *et al.*, Rev. Sci. Instrum. **85**, 103504 (2014).
[32]V. Y. Glebov *et al.*, Rev. Sci. Instrum. **81**, 10D325 (2010).
[33]C. K. Li *et al.*, Phys. Plasmas **7**, 2578 (2000).
[34]H. G. Rinderknecht *et al.*, Rev. Sci. Instrum. **83**, 10D902 (2012).
[35]H. G. Rinderknecht *et al.*, Rev. Sci. Instrum. **85**, 11D901 (2014).
[36]S. F. Khan *et al.*, Proc. SPIE **8505**, 850505 (2012).
[37]F. H. Séguin *et al.*, Rev. Sci. Instrum. **75**, 3520 (2004).
[38]J. L. DeCiantis *et al.*, Rev. Sci. Instrum. **77**, 043503 (2006).
[39]F. H. Séguin *et al.*, Phys. Plasmas **13**, 082704 (2006).
[40]A. L. Meadowcroft *et al.*, Rev. Sci. Instrum. **79**, 113102 (2008).
[41]B. Bachmann *et al.*, Rev. Sci. Instrum. **85**, 11D614 (2014).